

THE INTERNAL STRUCTURE OF MESOSCALE PRECIPITATION FEATURES
IN EXTRATROPICAL CYCLONIC STORMS

Thomas J. Matejka and Robert A. Houze, Jr.

Department of Atmospheric Sciences
University of Washington
Seattle, Washington

1. INTRODUCTION

From studies utilizing radar and raingage data it is now well established that the precipitation associated with extratropical cyclonic storms is often concentrated in mesoscale areas. These mesoscale precipitation areas frequently exhibit a banded structure. (See Browning, 1974; Harrold and Austin, 1974; Houze *et al.*, 1976a.)

Although some physical insights have been gained as to the nature of these mesoscale features, most studies have concentrated on describing the gross structure and kinematics of the mesoscale precipitation pattern. In particular, a good understanding of the rain- and snow-producing processes within the mesoscale features has not yet been achieved.

One of the principal aims of the CYCLES (Cyclonic Extratropical Storms) PROJECT, operated by the Cloud Physics Group at the University of Washington, is to investigate precipitation mechanisms in cyclonic storms. In this paper we present some findings on the microphysical structure of mesoscale precipitation features deduced from airborne measurements obtained in the CYCLES PROJECT. In another paper in these preprints (Hobbs *et al.*, 1976), the internal structure of mesoscale precipitation bands is investigated using radar data.

2. TYPES OF DATA

Six types of data were obtained during the field study:

(a) Synoptic maps and hourly observations were received on the standard facsimile and teletype circuits. Supplemental surface measurements were collected by our group.

(b) Cloud imagery from the NOAA SMS-2¹ satellite was obtained every half-hour.

(c) A rain gage mesonet network was employed (Houze *et al.*, 1976a and b).

(d) Rawinsondes were launched from a station at intervals of 45 min to 3 h.

(e) Radar data for this study were obtained with the University of Washington's (UW) search radar (wavelength 3.2 cm, beamwidth 1°, peak power 250 kW) and the National Center for Atmospheric Research (NCAR) CP-3 radar (wavelength 5.45 cm, beamwidth 1°, peak power 338 kW). The UW search radar provided quantitized PPI displays of radar reflectivity over a maximum range of 80 km. The NCAR CP-3 radar provided only limited measurements during some of the storm periods discussed in this paper.

(f) Airborne thermodynamical, dynamical, and microphysical measurements were obtained with the University of Washington's converted Douglas B-23 cloud physics research aircraft. (See Hobbs *et al.*, 1975, for a more detailed description of the aircraft observational system.) The aircraft data referred to in this paper include:

--Cloud liquid water content measured by a Johnson-Williams instrument.

--Ice particle concentrations using the UW optical ice particle counter (Turner *et al.*, 1976).

--Particle replication using a Meteorology Research, Inc., Continuous Formvar Particle Replicator.

3. ANALYTICAL PROCEDURES

Mesoscale precipitation features were identified using data from the rain gages and radars. The leading and back edges of these features were traced across the area of the field study in southwestern Washington state. The data collected from the aircraft were plotted as a function of altitude and of distance perpendicular to the moving edges of the features, producing the cross sections through the features shown in Figs. 2-6. A key to the symbols used is presented in Fig. 1.

CLOUD LIQUID WATER CONTENTS	
•	.10 - .20 g m ⁻³
●	.25 - .50 g m ⁻³
⦿	.55 - .95 g m ⁻³
⊙	≥ 1.00 g m ⁻³
ICE PARTICLE CONCENTRATIONS	
+	.5 - 2 l ⁻¹
x	2 - 4 l ⁻¹
*	4 - 8 l ⁻¹
⊕	8 - 16 l ⁻¹
⊗	16 - 32 l ⁻¹
⊛	32 - 64 l ⁻¹
⊠	≥ 64 l ⁻¹
RAIN INTENSITIES	
VL	very light
L	light
M	moderate
H	heavy

Fig. 1. Symbols used in Figs. 2-6.

The microphysical fields shown in the figures depict in a general manner the variations in the parameters through the features as well as the magnitudes of the quantities. The actual data are of far greater resolution along the flight path than it has been possible to show. The parameters measured on the aircraft were printed out in analog format and reduced digitally in 12 s averages. (In 12 s the aircraft travels approximately 0.7 km.)

The cloud configurations depicted in the cross sections were based on cloud sketches drawn on a time-height graph during each flight. The configurations shown in

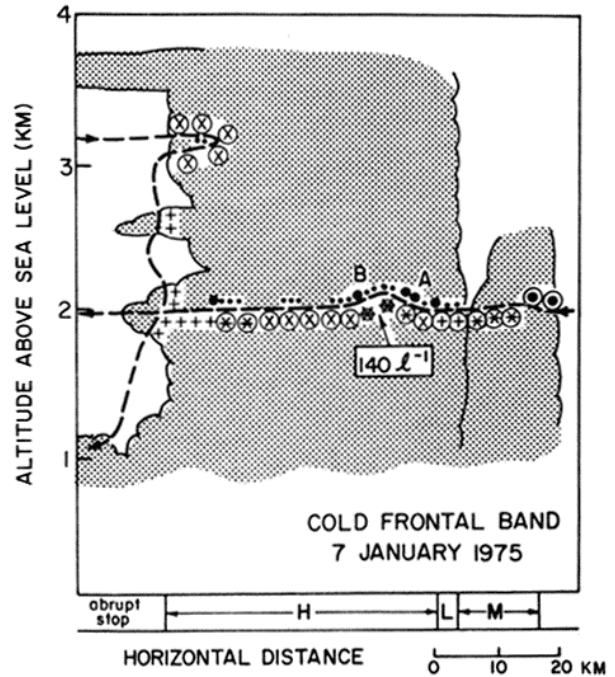


Fig. 2. Cross section through mesoscale cold frontal band. Cloud configurations are indicated by scalloped outlines and shading. The paths of the aircraft through the clouds are shown. Cloud microphysical parameters along the aircraft paths are explained in Fig. 1. Maximum observed ice crystal concentrations are indicated in boxes. The rainfall record is summarized at the bottom of the figures and is explained in Fig. 1. The leading edge of the band is on the right.

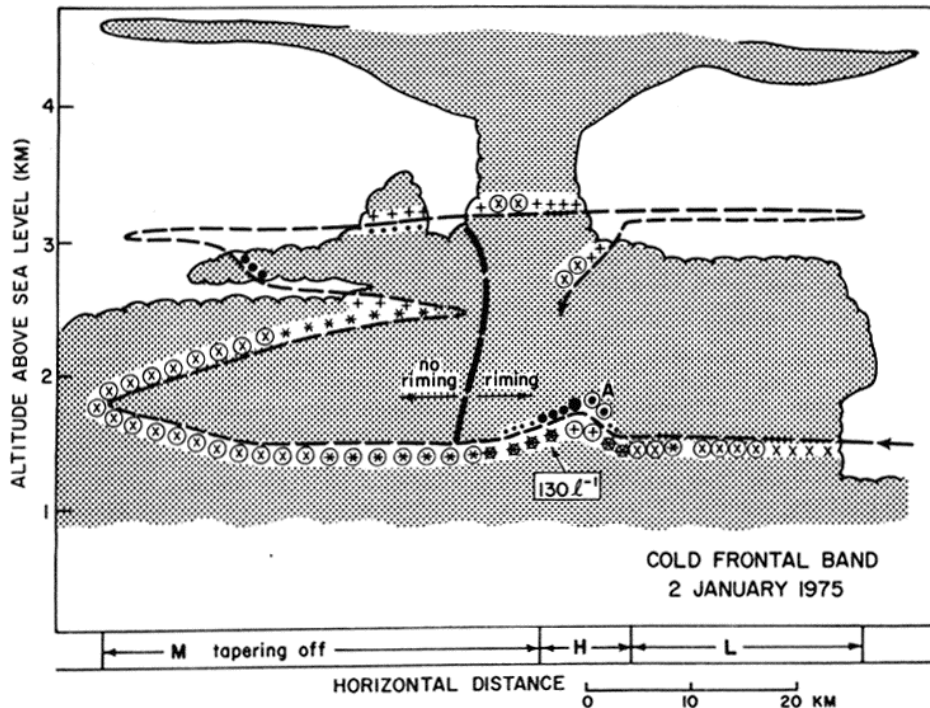


Fig. 3. Cross section through cold frontal band. Format same as Fig 2.

Figs. 2-6 were determined by transforming the original sketches into the moving coordinate systems of the mesoscale features.

4. DISCUSSION OF THE CROSS SECTIONS

The UW Cloud Physics group has gathered intensive data from approximately 20 mesoscale precipitation features. Six features have been selected for presentation here.

a. Three cold frontal bands

Cross sections through mesoscale cold frontal bands on 7 January 1975, 2 January 1975, and 16 December 1974 are shown in Figs. 2-4. The band of 7 January 1975 (Fig. 2) arrived with the leading edge of the cold air mass aloft in a warm occlusion, while the other two bands (Figs. 3-4) were associated with the frontal zones of ordinary cold fronts extending down to ground level.

The precipitation which was received at the ground with the passage of the three cold frontal bands is summarized at the bottoms of Figs. 2-4. Although the precipitation rates for each band varied considerably from station to station (with stations along the Pacific coast generally receiving greater amounts than inland stations), the shapes of the precipitation traces were similar among the stations. In the warm occlusion case (Fig. 2) the period of precipitation from the cold frontal band was relatively brief (lasting 20-40 min); the intensity reached maxima from 6 to 36 mm h⁻¹, and the rainfall then diminished rather quickly and stopped abruptly. In the cold frontal cases (Figs. 3-4) the precipitation was characterized by a short, initial burst of rain (peaking between a few and 30 mm h⁻¹) which was followed by a long period of lighter rain which tapered off slowly.

The patterns of microphysical quantities measured by the aircraft as it traversed the three cold frontal bands were similar in several ways. Large amounts of cloud liquid water were found toward the leading edges of the bands (indicated by the letter A in Figs. 2-4), nearly over the points where heavy precipitation began. Extensive regions of ice were present throughout the cloud bands. The largest numbers of ice particles were found in regions adjacent to the regions of highest cloud liquid water content; the peak ice concentrations are indicated in the figures. In Figs. 3-4 the ice particle concentrations were clearly depressed in the regions where the cloud liquid water content reached a maximum. A similar situation can also be seen in Fig. 2 in the smaller cloud element building at the leading edge of the main cloud band. This suggests that strong lifting and new condensation were taking place in those regions of highest cloud liquid water content at letter A in each figure, where the aircraft, attempting to fly a level flight pattern, was lifted markedly by an updraft. Using the deflections of the aircraft to calculate the magnitudes of the updrafts yield values of about 2.1 m s⁻¹ over 35 s of flight time (2 km of horizontal distance) in Fig. 2 and 2.7 m s⁻¹ over 47 s of flight time (3 km of horizontal distance) in Fig. 3. An updraft was also observed in the building cloud

element at the leading edge of the main cloud band in Fig. 2; the updraft in this element was 2.4 m s⁻¹ over 35 s of flight time (2 km of horizontal distance). Quantitative information on the updraft in Fig. 4 is not available; however, the similarity in the liquid water field of the cloud structure in Fig. 4 to that in Figs. 2-3 suggests that a comparable updraft was present. The magnitudes of the updrafts and the amounts of cloud liquid water present in them imply that the lifting taking place was unstable.

In the zone of strong lifting at letter A in Fig. 2 the cloud liquid water content, although comparable in magnitude to that found at letter B, was associated with almost twice the number of droplets (2470 cm⁻³) than were present at letter B (240 cm⁻³), indicating higher supersaturations and the apparent newness of the drop size spectrum in the core of the updraft.

Considerable riming occurred on the ice particles throughout the upper-level cold frontal band in Fig. 2 and in the leading portions of the surface cold frontal bands in Figs. 3-4. This was particularly clear-cut for the case shown in Fig. 3, and is indicated in the figure. Aggregates of ice crystals also tended to be largest and most abundant in these regions. Since these regions of the cloud were all situated over the heavy precipitation on the ground, riming and aggregation appear to have been important growth mechanisms for the most intense precipitation accompanying the bands. Riming and aggregation tended to be present in lesser degrees in the back portions of the bands in Figs. 3-4. This part of the cloud is associated with lighter precipitation on the ground.

The patterns of cloud liquid water, ice particle concentrations, and riming described here have much in common with the cold-frontal band described by Hobbs *et al.* (1975).

b. A warm frontal feature

A cross section through a large mesoscale feature which existed in a warm frontal zone on 7 January 1975 is shown in Fig. 5. The feature was identified by a 1.5 h period of very steady precipitation at the ground; rainfall rates were a few millimeters per hour.

Above the zone where rainfall occurred, the cloud consisted solely of modest concentrations of ice crystals (4-16 l⁻¹). At the back edge of the feature, however, behind the zone of precipitation, the cloud was composed of liquid water in amounts typical of stratiform lifting (up to 0.2 g m⁻³); almost no ice was present there. This indicates the importance of ice-phase growth to the production of precipitation in this warm frontal feature.

Riming was observed infrequently throughout the cloud, and then only slightly. Aggregation, however, was occurring in the leading half of the feature, and is indicated in Fig. 5. Aggregates up to 5 mm in diameter were observed. Since the winds relative to the cloud system were blowing from the back edge toward the leading edge (left to right in Fig. 5), the leading portion of the cloud probably consisted of the oldest cloud

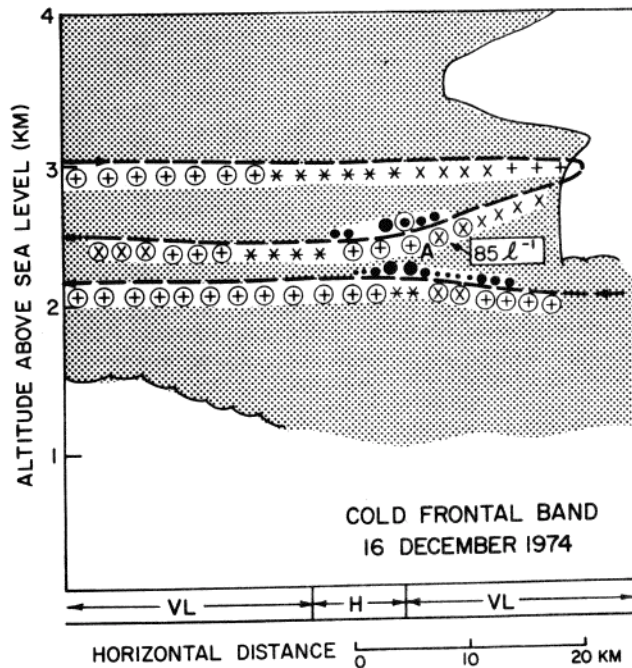


Fig. 4. Cross section through cold frontal band. Format same as Fig. 2.

particles. Fig. 5 also shows that the ice particle concentrations became 4 to 8 times lower in the region of the cloud where significant aggregation was occurring. This implies that, in the older region of the cloud, aggregation was a dominant growth mode which more than offset the amount of new crystal formation which may have been taking place.

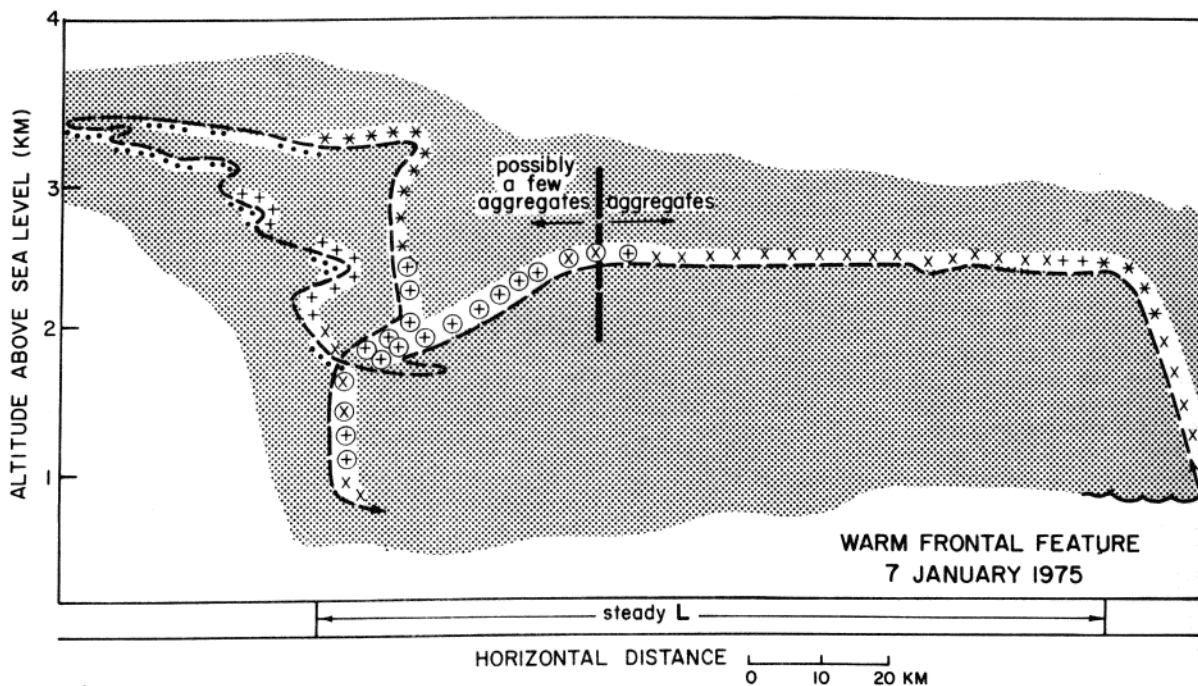


Fig. 5. Cross section through warm frontal feature. Format same as Fig. 2.

In the part of the cloud where aggregates were not observed, ice crystals had attained sizes up to 200-600 μm ; these can be attributed to depositional growth which appears to play a significant role in precipitation production in this cloud feature.

c. Two warm-sector bands

A cross section through two parallel warm-sector bands of 16 December 1974 are shown in Fig. 6. Peak rainfall rates at the ground from these bands were 4 to 6 mm h^{-1} .

These bands were in several respects qualitatively similar to the intense, prefrontal squall lines which are observed over the central United States. The warm-sector bands shown in Fig. 6 were aligned parallel to the approaching cold front, but were moving forward at a speed greater than the speed of the cold front. The visual appearance of the approaching bands was very reminiscent of the ominous bank of clouds which heralds a squall line. As the precipitation arrived from the warm-sector bands, the wet-bulb potential temperature at the surface decreased markedly, indicating the possibility of a precipitation-induced downdraft.

Fig. 6 shows that the leading band consisted of both ice and cloud liquid water, and the visual appearance of the cloud suggested that it was actively convective. The second band, however, was almost totally glaciated at the flight level, with greater concentrations of ice than were measured in the leading band. Although significant riming was detected in both features, large aggregates were present in the second band, while no aggregates were observed in the leading band. These microphysical observations, as well as the shape of the clouds in Fig. 6, indicate that the leading band was a developing feature, while the second band was a much older, perhaps

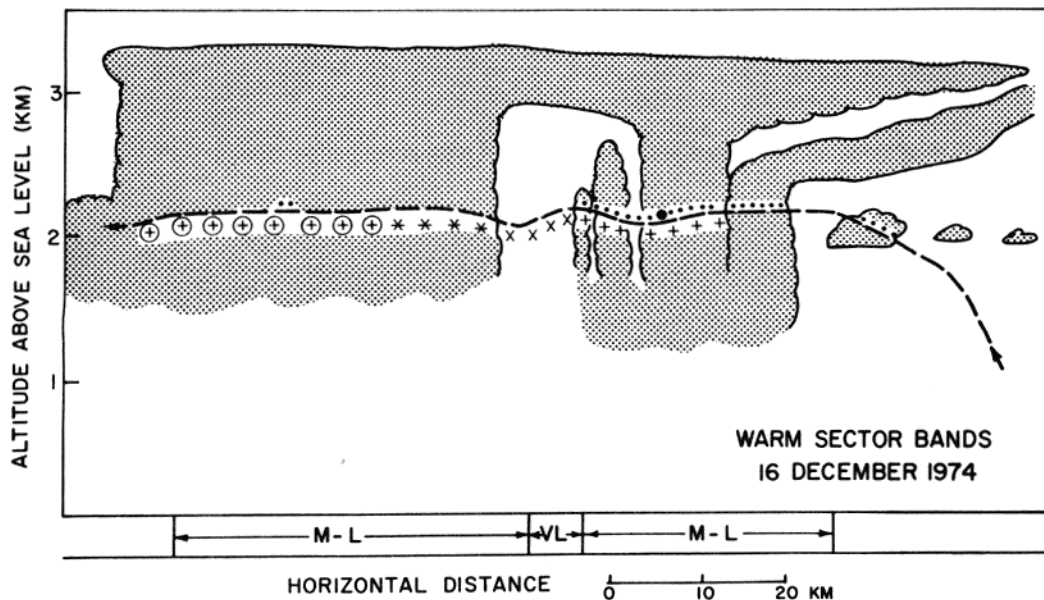


Fig. 6. Cross section through two warm-sector bands. Format same as Fig. 2.

decaying, one. This behavior is somewhat similar to that of intense convective storms in the central U.S. where new cells develop ahead of the older system (Dennis *et al.*, 1970; Browning *et al.*, 1976).

5. SUMMARY OF RESULTS

Examples of three mesoscale cold-frontal bands, a warm-frontal feature, and two warm-sector bands have been presented, and measurements of their internal microphysical structures have been described. Some conclusions can now be drawn concerning the means by which precipitation developed within them.

Although differences were observed among the mesoscale features discussed, it is important to observe that in all cases precipitation at the ground was associated with the presence of ice in the clouds above. Understanding the ice phase is unquestionably essential to understanding precipitation generation in these mesoscale features.

In all the features discussed here, the role of aggregation of ice particles seemed to be significant. In the cold frontal bands (Figs. 2-4) riming and aggregation were both in evidence above the zones of heaviest precipitation. Where the precipitation was lighter, immediately behind the belt of heavy precipitation in Figs. 3-4, riming and aggregation decreased significantly. Riming appeared to play an important role in the warm-sector bands (Fig. 6), while depositional growth appeared to be more important than riming in the warm frontal precipitation (Fig. 5).

6. CONCLUSION

The results presented here were obtained largely by analyzing microphysical data collected aboard the University of Washington's research aircraft, and the distributions and characteristics of liquid and ice particles measured within the mesoscale cloud features have given some indication of factors which may be important in the production of precipitation in these features.

The study of mesoscale precipitation structures and processes can be expanded significantly by supplementing the data obtained along aircraft flight paths with simultaneous radar measurements which cover large regions surrounding the aircraft. Houze *et al.* (1976b) and Hobbs *et al.* (1976), for example, have used vertically-pointing Doppler radar measurements to deduce particle growth and evaporation processes both above and below the melting layer in mesoscale rainbands of occluded cyclones. As part of the CYCLES PROJECT we are now conducting field studies with expanded radar coverage, using a vertically-pointing Doppler radar to provide continuous time-height coverage, the UW search radar to track mesoscale precipitation features, and the NCAR CP-3 radar operating in a series of conical, RHI, and vertically-pointing modes to provide extensive reflectivity and velocity data. Coordination of multilevel aircraft penetrations with this detailed radar coverage should lead to a more comprehensive picture of the internal structure of mesoscale precipitation features and a better understanding of the physical mechanisms of precipitation in cyclonic storms.

ACKNOWLEDGEMENTS

We thank Professor Peter V. Hobbs, Director, and the members of the Cloud Physics Group at the University of Washington who participated in the field program and who assisted in the data reduction and analysis. This re-research was sponsored by the Atmospheric Research Section (Meteorology Program) of the National Science Foundation under Grant ATM-74-14726-A02.

REFERENCES

- Browning, K. A., 1974: Mesoscale structure of rain systems in the British Isles. J. Meteor. Soc. Japan, 50, 314-327.
- _____, J. C. Fankhauser, J.-P. Chalon, P. J. Eccles, R. G. Strauch, F. H. Merrem, D. J. Musil, E. L. May, and W. R. Sand, 1976: Structure of an evolving hailstorm, part V: synthesis and implications on hail growth and hail suppression. Mon. Wea. Rev., 104, 603-610.
- Dennis, A. S., C. A. Schock and A. Koscielski, 1970: Characteristics of hailstorms of western South Dakota. J. Appl. Meteor., 9, 127-135.
- Harrold, T. W., and P. M. Austin, 1974: The structure of precipitation systems - a review. J. de Rech. Atmosph., 8, 41-57.
- Hobbs, P. V., R. A. Houze, Jr., and T. J. Matejka (1975); The dynamical and Microphysical structure of an occluded front and its modification by orography. J. Atmos. Sci., 32, 1542-1562.
- _____, J. D. Locatelli and R. R. Weiss, 1976: Wave-like precipitation bands and precipitation cells in an occluded frontal system. Preprints 17th Radar Meteorology Conference, Seattle, Amer. Meteor. Soc.
- Houze, R. A., Jr., P. V. Hobbs, K. R. Biswas, and W. M. Davis, 1976a: Mesoscale rainbands in extratropical cyclones. Mon. Wea. Rev., in press.
- _____, J. D. Locatelli, and P. V. Hobbs, 1976b: Dynamics and cloud microphysics of the rainbands in an occluded frontal system. J. Atmos. Sci., in press.
- Turner, F. M., L. F. Radke, and P. V. Hobbs, 1976: Optical techniques for the counting of ice particles in mixed phase clouds. Atmos. Technol., in press.